Parameter Estimation For Generalized Extreme Value Distribution In Rainfall Forecasting: A Case Study Of Bangkok

Autcha Araveeporn* and Paradorn Sukpan

Department of Statistics, School of Science, King Mongkut's Institute of Technology Ladkrabang, Bangkok, Thailand

** Corresponding author. E-mail: autcha.ar@kmitl.ac.th*

Received: Jul. 25, 2024; Accepted: Feb. 06, 2025

This study aims to compare efficiency methods for the estimated parameter of Generalized Extreme Value Distribution (GEVD), which consists of location, scale, and shape parameters. The parameter estimation employs the maximum likelihood (ML), generalized maximum likelihood (GML), Bayesian, and L-moments methods. The data is generated through simulation data in Gumbel, Fréchet, and Weibull distributions verified by shape parameters. The performance of these methods is evaluated using the minimum mean squared error (MSE) and mean absolute percentage error (MAPE). The results indicate that the Bayesian, ML, and GML methods consistently achieve the lowest MSE values, such as 0.0120 for location, 0.0066 for scale, and 0.005 for shape parameters when the sample size is 100 of the Gumbel distribution. In the real data application using 29 years of Bangkok rainfall data (1994-2023), the GEVD model estimated return levels for 2 to 9 years, with MAPE values ranging from 32.57% to 56.92% across different stations. The findings suggest that ML and GML methods outperform others in simulated and real-world applications. The proposed approach provides accurate and reliable forecasts of extreme rainfall, which are crucial for Bangkok's urban planning and flood risk management.

Keywords: generalized extreme value distribution; generalized maximum likelihood; L-moments

http://dx.doi.org/10.6180/jase.202512_28(12).0009

1. Introduction

Inferential statistics is a critical branch that focuses on making statistics or estimators based on a sample of data to infer about a parameter population. An estimator is a sample function, while an estimate is the estimated value of an estimator obtained when a sample is taken [1]. Inferential statistics is essential for making data-driven decisions in the face of uncertainty that extends beyond the immediate data, enabling us to understand and act upon the patterns and trends within data. The fundamental concepts of inferential statistics are focused on estimation and hypothesis testing across various fields such as Holms and Walker [2], Siebert [3], Cal et al. [4], Chong et al. [5], and Wadsworth and Campbell [6].

There are two primary types of parameter estimation: point and interval estimations. Point estimation offers a single value as an estimate of a population parameter. In contrast, interval estimation generates a range of values, known as a confidence interval, within which the parameter is expected to fall. Various methods for parameter estimation include the moments, maximum likelihood, and Bayesian methods [1]. By employing various estimation methods and understanding key concepts like bias, consistency, efficiency, and sufficiency, statisticians and researchers can accurately interpret population characteristics [7–9].

Extreme Value Theory (EVT) is a field of statistics focusing on extreme deviations from the median of probability distributions. These are the values in a dataset that are sig-

nificantly higher than the majority of the data points. These extreme values represent the tail ends of the distribution and are critical for understanding rare but impactful events such as floods, heatwaves, and financial crises. The benefit of extreme value theory is that the origin distribution and its cumulative distribution do not need to be known as the distribution of the extremes asymptotically approaches a known distribution [10]. Block maxima are the maximum values within a specified data block, such as the monthly flood volume and the yearly highest daily temperature. Tabari [11] studied extreme value theory to confirm the theoretical foundation for the statistical modeling of extreme hydrological events using block maxima. Raiman et al. [12] utilized climate variables, including air temperature, wind speed, maximum and minimum temperatures, and rainfall, to determine the magnitude of risk by applying block maxima. These variables are used to model the distribution of block maxima, which is one of the three types of distributions in the Generalized Extreme Value Distribution (GEVD) family.

The GEVD is widely used in EVT to model the distribution of block maxima over a specified period. The GEVD incorporates three types of distributions, Gumbel, Fréchet, and Weibull, depending on the tail behavior of the underlying data. Accurately estimating GEVD parameters, including location, scale, and shape, is crucial for reliable modeling and forecasting of extreme events. Recent advancements in EVT have introduced novel parameter estimation techniques and more robust computational methods, such as improved numerical optimization algorithms for maximum likelihood [13, 14], L-moments [15], and Bayesian methods [14, 16, 17].

The Maximum Likelihood (ML) method is a powerful statistical tool for estimating parameters based on the probability distribution by maximizing the likelihood function. When applied to the GEVD, ML aims to approximate the parameters that maximize the likelihood function, representing the probability of observing the given sample. Numerical optimization is necessary because the log-likelihood function of the GEVD is often complex and does not have a closed-form solution. Louzaoui and Arrouchi [18] studied the existence and consistency of the maximum likelihood method via the extreme value index based on k-record values.

The Generalized Maximum Likelihood (GML) method extends the traditional ML estimation. It is beneficial when the likelihood equations are complex and cannot be solved analytically. The GML uses numerical methods to maximize the likelihood function, performing a robust framework for parameter estimation in generalized extreme value analysis. Adlouni et al. [19] developed efficient estimation methods for using the GEVD for quantile estimation in the presence of nonstationary, which was generally done with the ML estimation method.

The Bayesian method provides a robust framework for parameter estimation, incorporating prior knowledge and observed data to form a comprehensive analysis. The Bayesian approach of GEVD allows for integrating prior beliefs about the parameters with the likelihood derived from the data, leading to a posterior distribution that reflects both sources of information. Yoon et al. [14] developed a comprehensive Bayesian estimation approach to GEVD, incorporating a semi-Bayesian framework of GML to fully leverage several advantages of the Bayesian approach, particularly in uncertainty analysis. Markov Chain Monte Carlo (MCMC) methods are a class of algorithms used to sample from probability distributions by constructing a Markov chain with the desired distribution as its equilibrium posterior distribution. The application of GEVD, the MCMC method, employs a powerful tool for estimating the distribution parameters, particularly in a Bayesian framework. Krüger et al. [20] used the Bayesian inference to predict distributions generated via Markov chain Monte Carlo or related algorithms.

L-moments are statistical measures used to summarize the probability distributions of data, offering a robust alternative to conventional moments for parameter estimation. This method is exhibited in the form of linear combinations based on order statistics, offering more robustness to outliers and better efficiency in small samples. Furthermore, L-moments provide a straightforward and reliable method for characterizing the distribution's shape, scale, and location parameters. Khan et al. [21] developed regional frequency methods based on L-moments and partial L-moments to derive generalized extreme value, generalized logistic, generalized normal, and generalized Pareto distributions.

Choosing the appropriate method for parameter estimation depends on various factors, including the sample size, computational resources, and the availability of prior information. In practical applications, ML method is often preferred for its efficiency and accuracy, especially with large datasets that extend to GML method. However, the L-moments can be helpful for a quick and straightforward estimation, while Bayesian estimation is valuable when incorporating prior knowledge or dealing with small sample sizes. However, these methods must be applied to real-world climate data and assessed for their robustness under non-stationary conditions induced by climate change. This study aims to address these gaps by comparing the effi-

ciency of parameter estimation methods, including MLE, Generalized Maximum Likelihood (GML), Bayesian, and L-moments, in forecasting maximum rainfall events in Bangkok.

Bangkok, Thailand's bustling capital, is prone to extreme weather events and hefty rainfall during the monsoon season. Forecasting maximum rain volume is crucial for urban planning, flood management, and disaster preparedness. Tanprayoon et al. [22] presented an extension of the GEVD based on the T-X family of distributions: the Gompertz-generated family of distributions, which makes the existing distribution more flexible. This extension, called the Gompertz-general extreme value distribution, was used to estimate the return levels of rainfall values in Lopburi Province. Martins and Stedinger [23] estimated the three parameters of GEVD, which have broad applications in describing yearly floods, rainfall volume, speeding wind, and other maximum values. Ng et al. [24] studied the GEVD to identify the best-fit probability distribution for monthly and annual extreme temperatures in hydrological studies and event forecasting. Generalized extreme value analysis offers a robust statistical approach for modeling and predicting extreme rainfall events, allowing us to estimate the return levels of specific magnitudes of rainfall expected to occur within a given return period.

The objectives of this study are directly linked to practical applications in urban infrastructure and flood mitigation planning. Accurate estimation of extreme rainfall levels is essential for designing drainage systems, optimizing flood control measures, and developing early warning systems to mitigate the impact of extreme weather events. With Bangkok experiencing increasing rainfall intensities due to climate variability, this research provides valuable insights for urban planners and policymakers to enhance resilience against extreme weather conditions.

This study comprehensively compares parameter estimation methods for GEVD under varying sample sizes and data characteristics, evaluates their performance using real-world rainfall data, and provides recommendations for urban planning based on predicted extreme rainfall levels. The findings contribute to improved decision-making in urban flood management and disaster preparedness.

2. Materials and methods

The Generalized Extreme Value Distribution (GEVD) is suitable for analyzing extreme values over specified intervals, such as weekly, monthly, or yearly. The analysis involves selecting the maximum value from each time interval of interest. This approach uses the block maxima method, a widely used and appropriate technique for data exhibiting GEVD characteristics.

Let $X_1, \ldots, X_n$ be the independent random variable and denote the cumulative distribution function as $F(x;\theta)$. The maximum value of the random variable is defined as $X_{(n)} = \max(X_1, \ldots, X_n)$ and is supposed GEVD as $X \sim \text{GEVD}(\mu, \sigma, \xi)$. The maxima of the sequence, when properly normalized, converges in distribution to a limiting form. This is expressed as $P\left(\frac{X_{(n)}-a_n}{b_n} \leq x\right) \to F(x;\theta)$, as n $\to \infty$, where a_n and $b_n > 0$ are normalizing sequences and $F(x;\theta)$ is the limiting extreme value distribution.

According to the Fisher-Tippett-Gnedenko theorem [25], the possible limit distributions for block maxima belong to one of three families: Gumbel, Fréchet, and Weibull, which can all be encompassed the cumulative distribution function of GEVD and represented in Eq. (1) as

$$F(x;\mu,\sigma,\xi) = \begin{cases} \exp\left\{-\left(1+\xi\left(\frac{x-\mu}{\sigma}\right)\right)^{-1/\xi}\right\} & ,\xi \neq 0 \\ \exp\left\{-\exp\left(\frac{x-\mu}{\sigma}\right)\right\} & ,\xi = 0 \end{cases} \tag{1}$$

The derivation of the Generalized Extreme Value Distribution (GEVD) follows from the extreme value theorem, which states that the distribution of block maxima converges to a limiting form under specific conditions. The derivation details can be found in Coles [25] and Beirlant et al. [26], which provide comprehensive discussions on the asymptotic behavior and parameter estimation techniques. The probability distribution function [26] is given by

$$f(x;\mu,\sigma,\xi) = \begin{cases} \frac{1}{\sigma}\left[1+\xi\left(\frac{x-\mu}{\sigma}\right)\right]^{(-1/\xi)-1} \\ \quad \exp\left\{-\left(1+\xi\left(\frac{x-\mu}{\sigma}\right)\right)^{-1/\xi}\right\} & ,\xi \neq 0 \\ \frac{1}{\sigma}\exp\left(\frac{x-\mu}{\sigma}\right)^{-1}\exp\left\{-\exp\left(\frac{x-\mu}{\sigma}\right)\right\} & ,\xi = 0 \end{cases} \tag{2}$$

where $\left\{1+\xi\left(\frac{x-\mu}{\sigma}\right)\right\} > 0, -\infty < \mu, \xi < \infty, \sigma > 0.$

The GEVD is characterized by location (μ), scale (σ), and shape (ξ) parameters. These parameters are interpreted as location parameters that determine the central tendency or the location of the distribution. Scale parameter controls the dispersion or the scale of the distribution.

The shape parameter governs the tail behavior of the distribution when different values correspond to different types of GEVD. Depending on the shape's parameter, the GEVD encompasses three types such as Gumbel distribution ($\xi = 0$), Fréchet distribution ($\xi > 0$), and Weibull distribution ($\xi < 0$). Understanding these parameters is essential for practical applications, such as designing flood control systems, planning drainage infrastructure, and developing disaster mitigation strategies based on estimated return levels. Applying GEVD to historical rainfall data can estimate return levels over different time horizons, providing valuable insights into the probability and magnitude

of extreme rainfall events crucial for urban planning and climate adaptation efforts.

The GEVD's suitability for modeling extremes derives from extreme value theory, which states that the distribution of maxima converges to one of three types, depending on the tail behavior of the underlying distribution. The shape parameter (ξ) plays a critical role in defining the tail behavior of the distribution and determines which type of GEVD applies to Gumbel distribution as the light-tail data, where extreme values decay exponentially, and is often used for environmental data, like annual maximum rainfall, where extreme values are not overly large. Fréchet distribution is suitable for heavy-tailed distributions. This form captures data where extreme events are significantly large, making it applicable to fields where the probability of extreme, impactful events is substantial. Weibull Distribution performs on bounded data with a finite upper limit on possible extreme values. In the context of rainfall, this distribution would be relevant if the physical conditions naturally limit the maximum rainfall that can occur. The interesting methods for estimating the parameters of GEVD are maximum likelihood, generalized maximum likelihood, Bayesian, and L-moments methods.

2.1. Maximum Likelihood (ML) Method

ML method is the most widely used method for estimating the parameters of the GEVD. This method mentions to approximate the parameter values that maximize the likelihood function, representing the probability by observing the given data under the assumed model. The steps for parameter estimation are as follows:

Step 1: Consider the GEVD of the random variable from Eq. (2).

Step 2: Construct the likelihood function of the random variable based on the GEVD $(\xi \neq 0)$ that $L(\mu, \sigma, \xi)$. Therefore as

$$L(\mu,\sigma,\xi) = \frac{1}{\sigma^n}\prod_{i=1}^{n}\left[1+\xi\left(\frac{x_i-\mu}{\sigma}\right)\right]^{(-1/\xi)-1} \exp\left\{-\sum_{i=1}^{n}\left(1+\xi\left(\frac{x_i-\mu}{\sigma}\right)\right)^{-1/\xi}\right\} \tag{3}$$

The score function of the location parameter:

$$\frac{\partial L}{\partial \mu} = \sum_{i=1}^{n}\left(\frac{1}{\xi\sigma}\right)\left(1+\xi\frac{x_i-\mu}{\sigma}\right)^{-1} - \frac{1}{\sigma}\sum_{i=1}^{n}\left(1+\xi\frac{x_i-\mu}{\sigma}\right)^{-(1+1/\xi)} = 0$$

The score function of the scale parameter:

$$\frac{\partial L}{\partial \sigma} = -\frac{n}{\sigma} + \frac{1}{\sigma}\sum_{i=1}^{n}\left(1+\xi\frac{x_i-\mu}{\sigma}\right)^{-1}\left(\frac{x_i-\mu}{\sigma}\right) - \frac{1+1/\xi}{\sigma}\sum_{i=1}^{n}\left(1+\xi\frac{x_i-\mu}{\sigma}\right)^{-(1+1/\xi)} = 0$$

The score function of the shape parameter:

$$\frac{\partial L}{\partial \xi} = \sum_{i=1}^{n}\left(\frac{x_i-\mu}{\sigma}\right)\left(1+\xi\frac{x_i-\mu}{\sigma}\right)^{-1}\left(1-\frac{1}{\xi^2}\ln\left(1+\xi\frac{x_i-\mu}{\sigma}\right)\right) - \sum_{i=1}^{n}\left(1+\xi\frac{x_i-\mu}{\sigma}\right)^{-(1+1/\xi)} = 0$$

Step 3: Take the logarithm of the likelihood function from Eq. (3) to obtain the log-likelihood function of GEVD, which is called $l(\mu, \sigma, \xi)$. It can be written by

$$l(\mu,\sigma,\xi) = -n\log(\sigma) - \left(1+\frac{1}{\xi}\right)\sum_{i=1}^{n}\log\left[1+\xi\left(\frac{x_i-\mu}{\sigma}\right)\right] - \sum_{i=1}^{n}\left(1+\xi\left(\frac{x_i-\mu}{\sigma}\right)\right)^{-1/\xi} \tag{4}$$

Step 4: Differentiate the log-likelihood function with respect to each parameter (μ, σ, ξ) to obtain the score equations. Then, the MLE estimators $(\hat{\mu}, \hat{\sigma}, \hat{\xi})$ are evaluated by

$$\frac{\partial l(\mu,\sigma,\xi)}{\partial \mu} = 0, \quad \frac{\partial l(\mu,\sigma,\xi)}{\partial \sigma} = 0, \quad \frac{\partial l(\mu,\sigma,\xi)}{\partial \xi} = 0$$

Taking partial derivatives to maximize the likelihood function is difficult due to the complexity of the equations, making it impossible to solve the likelihood equations analytically. Therefore, parameter estimation is performed using numerical analysis, precisely the Newton-Raphson method [27]. The likelihood equations for GEVD involve partial derivatives with respect to the μ, σ, and ξ. Including the ξ introduces a nonlinearity that makes the equations complex and, in most cases, prevents closed-form solutions. The functional form of the ξ affects the tail behavior, which is crucial for extreme value modeling, but this complexity also means that direct analytical solutions are not feasible. Due to this nonlinearity, iterative numerical methods are essential. The impact of the initial parameter selection on convergence is significant. If the starting values are too far from the optimal solution, the iterative procedure may require more iterations or even fail to converge. This study defined a tolerance level $\left(10^{-6}\right)$ to address this to determine when the iterative process should stop. The Newton-Raphson method refines the parameter estimates iteratively, adjusting based on the slope of the likelihood function until the difference between successive estimates is below the specified threshold. Sensitivity analysis was

conducted by varying the initial parameter values across a reasonable range and observing convergence patterns. The analysis indicated that starting values close to the empirical estimates resulted in faster convergence and more stable solutions. Additionally, multiple runs with different starting values were performed to ensure the global maximum of the likelihood function was attained

Newton-Raphson, a root-finding technique, is particularly suited for solving these equations. Approximating the solutions iteratively refines the parameter estimates at each step based on the slope of the likelihood function, adjusting until convergence is achieved. Accurate estimation is critical for distributions like GEVD, where the ξ governs the tail behavior and the risk of extreme events. Numerical optimization methods like Newton-Raphson provide a reliable approach to handling this complexity, making them indispensable for extreme value applications where traditional analytical solutions are insufficient.

When dealing with large datasets, the computational complexity of solving the likelihood equations increases significantly, mainly due to the shape parameter (ξ), which introduces non-linearity and sensitivity in the estimation process. The Newton-Raphson method, commonly used for parameter estimation, may require numerous iterations to achieve convergence, leading to high computational costs. To address these challenges, alternative optimization techniques such as quasi-Newton methods, expectation-maximization algorithms, or stochastic gradient descent can be employed to enhance efficiency. Additionally, parallel computing and subsampling strategies can reduce computational time while maintaining estimation accuracy.

The ML method for estimating GEVD parameters can be summarized as follows: construct the likelihood function based on this model, then simplify the process by taking the logarithm to form the log-likelihood function. Differentiate the log-likelihood with respect to each parameter to find where the function is maximized. Finally, these equations are solved, often using numerical methods like the Newton-Raphson method, to obtain the parameters' maximum likelihood estimator.

2.2. Generalized Maximum Likelihood (GML) Method

The GML method is a method used for parameter estimation in cases where the assumptions of the standard ML estimation are not met. ML method typically assumes that the data follow a specific distribution, such as the normal, binomial, or unknown distribution.

In contrast, GML assumes that the data follow a more flexible function that can accommodate a variety of data distributions, including nonparametric statistics. Some literature considers GML the nonparametric maximum likelihood estimator. The principle of GML is similar to that of ML: finding the parameters that maximize the generalized likelihood estimator. Methods such as empirical likelihood, quasi-likelihood, or estimating equations [28]. As shown below, they assigned a prior density to the shape parameter, assuming it follows a Beta distribution as

$$\pi(\xi) = \frac{(0.5+\xi)^{u-1}(0.5-\xi)^{v-1}}{B(u,v)}, \quad -0.5 \le \xi \le 0.5, \quad u = 6, v = 9 \tag{5}$$

where $B(u,v) = \frac{\Gamma(u)\Gamma(v)}{\Gamma(u+v)}$, the mean and variance are defined by $E(\xi) = -0.1$ and $\mathrm{Var}(\xi) = 0.015$. The informative prior of Beta distribution [23], derived from the geophysical prior, would likely provide narrower credible intervals, enhancing the robustness and reliability of the Bayesian inference. The Beta distribution is particularly suited as a prior distribution for the shape parameter because it is defined on a bounded interval, allowing control over the tail behavior in the GEVD model. By setting parameters for the beta distribution, the prior can represent various tail shapes, which is essential in extreme value modeling where tail heaviness is critical.

In this study, the Beta distribution for the shape parameter ($-0.5 \le \xi \le 0.5$) is bounded within a specific range, making it easier to control and interpret the tail behavior without risking extreme or non-physical values. This bounded nature aids in modeling realistic rainfall extremes, ensuring the resulting posterior distribution aligns with the prior knowledge of likely rainfall behaviors in extreme scenarios.

The parameter estimators of the GML method are similar to those of the ML method, with the generalized likelihood function in Eq. (3) being based on Bayesian theory, which combines prior distribution with new evidence to update beliefs or probabilities about an uncertain event, such as the beta distribution. It can be represented as follows:

$$GL(X;\mu,\sigma,\xi) = L(X;\mu,\sigma,\xi)\pi(\xi) \tag{6}$$

Therefore, the generalized log-likelihood function can be represented as and can be calculated from Eq. (6) by

$$l_G = \log\left(L\left(X \mid \theta_i\right)\right) + \log\{\pi(\xi)\} \tag{7}$$

The Hessian matrix [27] H is the matrix of second derivatives of the log-likelihood function with respect to the parameters: $H = \frac{\partial^2 l_G}{\partial\theta\partial\theta^T}$. The addition of the prior $\log\pi(\theta)$ modifies the curvature of the log-likelihood, impacting the elements of the Hessian matrix: $H = H_{\text{data}} + H_{\text{piac}}$, which $H_{\text{dta}} = \frac{\partial^2 \log(L(X|\theta_i))}{\partial\theta\partial\theta^T}$ comes from the likelihood function, and $H_{\text{pia}} = \frac{\partial^2 \log\{\pi(\xi)}{\partial\xi\partial\xi^T}$.

The parameter estimation procedure using the GMLE method for the GEVD consists of four steps as follows:

Step 1: Consider the probability distribution function of the random variable X from Eq. (2) and the prior probability $\pi(\xi)$ from Eq. (5).

Step 2: Construct the generalized likelihood function of the random variable based on the GEVD when $\xi \neq 0$ as

$$GL(\mu,\sigma,\xi) = \frac{1}{\sigma^n}\prod_{i=1}^{n}\left[1+\xi\left(\frac{x_i-\mu}{\sigma}\right)\right]^{(-1/\xi)-1} \exp\left\{-\sum_{i=1}^{n}\left(1+\xi\left(\frac{x_i-\mu}{\sigma}\right)\right)^{-1/\xi}\right\}\pi(\xi) \tag{8}$$

Step 3: Define the log-likelihood function of the random variable based on the GEVD as $l_G(\mu,\sigma,\xi)$, this can be represented as

$$l_G(\mu,\sigma,\xi) = -n\log(\sigma) - \left(1+\frac{1}{\xi}\right)\sum_{i=1}^{n}\log\left[1+\xi\left(\frac{x_i-\mu}{\sigma}\right)\right] - \sum_{i=1}^{n}\left(1+\xi\left(\frac{x_i-\mu}{\sigma}\right)\right)^{-1/\xi} + \log\{\pi(\xi)\} \tag{9}$$

Step 4: Estimate the parameters by taking the partial derivatives of the function obtained in Step 3, and the GMLE of $\hat{\mu},\hat{\sigma},\hat{\xi}$ can be derived from

$$\frac{\partial l_G(\mu,\sigma,\xi)}{\partial\mu}=0, \quad \frac{\partial l_G(\mu,\sigma,\xi)}{\partial\sigma}=0, \quad \frac{\partial l_G(\mu,\sigma,\xi)}{\partial\xi}=0$$

Due to the equations' complexity, taking partial derivatives to maximize the generalized log-likelihood function is difficult and complex, making solving the likelihood equations analytically impossible. Therefore, parameter estimation is performed using numerical analysis methods, specifically the Newton-Raphson method, similar to the ML approach [14].

The GML method extends the traditional ML approach by allowing for greater flexibility and the incorporation of prior information on Beta distribution, making it a powerful tool for estimating the parameters of the ML process.

2.3. Bayesian Method

Bayesian estimation incorporates prior information about the parameters in the form of prior distributions and updates this information using the observed data to obtain posterior distributions. In a Bayesian context, parameter estimation involves computing the posterior distribution of the parameters given the data. Markov Chain Monte Carlo (MCMC) methods [29] facilitate this by generating samples from the posterior distribution when direct analytical methods are infeasible. The Metropolis-Hastings (MH) algorithm [30] is the most widely used MCMC method, which is a general term for a family of Markov chain simulation algorithms useful for sampling from Bayesian posterior distributions [31]. It proposes new sample points and accepts or rejects them based on a specific probability criterion, ensuring the chain converges to the desired distribution.

The process of parameter estimation using the Bayesian method based on GEVD consists following steps:

Step 1: Define the posterior distribution of the GEVD parameters (μ,σ,ξ) given the observed data $x_1,x_2,\ldots,x_n$. It combines the likelihood function and the prior distributions of the parameters:

$$p(\mu,\sigma,\xi \mid x) \propto p(x \mid \mu,\sigma,\xi)p(\mu)p(\sigma)p(\xi) \tag{10}$$

where $p(x \mid \mu,\sigma,\xi)$ is a likelihood function, and $p(\mu), p(\sigma)$, and $p(\xi)$ are the prior distributions.

The appropriate priors for the GEVD parameters are $\mu \sim N\left(\mu_0,\sigma_0^2\right)$ or normal distribution, $\sigma \sim IG(a,b)$ or inverse-gamma distribution, and $\xi \sim U(a,b)$ or uniform distribution. Using a normal prior for location or scale parameters often leads to posterior distributions centered around expected values, but it might not adequately capture extreme variability in the shape parameter. For the scale parameter, an inverse-gamma prior helps capture higher levels of uncertainty by allowing a heavy tail, which is often necessary for extreme value modeling, where variability can be significant. A uniform prior for the shape parameter could illustrate the broadest range of outcomes, particularly useful if there is limited prior knowledge, and shows a baseline against which the informativeness of other priors can be compared.

This sensitivity analysis could involve comparing the posterior distributions of GEVD parameters across different priors, assessing convergence, and observing any shifts in the posterior mean or variance that different priors introduce. Such an analysis would demonstrate how Bayesian estimation is adaptable based on the information encoded in priors, thus reinforcing the robustness of the GEVD parameter estimation framework within the Bayesian context.

Step 2: Choose the initial value $\theta^{(0)} = \left(\mu^{(0)},\sigma^{(0)},\xi^{(0)}\right)$ from prior distribution and generate a proposed new state $\theta' = (\mu',\sigma',\xi')$ from a proposal distribution $q\left(\theta' \mid \theta^{(t)}\right)$.

Step 3: Compute the acceptance probability α :

$$\alpha = \min\left(1, \frac{p\left(\theta' \mid x\right) q\left(\theta^{(t)} \mid \theta'\right)}{p\left(\theta^{(t)} x\right) q\left(\theta' \mid \theta^{(t)}\right)}\right) \tag{11}$$

where $p(\theta \mid x)$ is the posterior distribution.

Step 4: Check convergence diagnostics: The Gelman-Rubin statistic [32], also known as the potential scale reduction factor $(\hat{R})$, is a diagnostic tool used to assess the

convergence of Markov Chain Monte Carlo (MCMC) simulations. It compares the variability within each MCMC chain to the variability between multiple chains to determine if they have converged to a common distribution. The formula for the Gelman-Rubin statistic is:

$$\hat{R} = \sqrt{\frac{\hat{V}}{W}} \tag{12}$$

where W is the within-chain variance as $W = \frac{1}{m}\sum_{j=1}^{m} s_j^2, s_j^2$ is the sample variance of chains j, and m is the number of chains. From Eq. (11), B is the between-chain variance as $B = \frac{n}{m-1}\sum_{j=1}^{m}\left(\bar{\theta}_j - \bar{\theta}\right)^2, \bar{\theta}_j$ is the mean of chain j, and $\bar{\theta}$ is the is the overall mean across all chains, and n is the number of samples per chain. The total variance estimate $\hat{V}$ is computed by $\hat{V} = \frac{n}{n-1}W + \frac{B}{n}$, then the $\hat{R}$ is close to one, indicating that the chains likely converged to the target distribution.

Step 5: Autocorrelation Plots:

Autocorrelation measures the correlation between samples at different steps in the chain. Low autocorrelation values suggest that the samples are relatively independent, which is crucial for accurate posterior estimation. Examining these plots helps ensure that the chain has sufficiently mixed and that the parameter estimates are reliable.

Step 6: Parameter estimation using posterior samples:

After convergence diagnostics confirm that the chain has reached stationarity, the posterior samples can be used to estimate the parameters by setting $\theta^{(t+1)} = \theta'$ with probability α; otherwise $\theta^{(t+1)} = \theta^{(t)}$, and compute the estimator $(\hat{\mu}, \hat{\sigma}, \hat{\xi})$ by mean θ'.

Using the Bayesian method gives us a more comprehensive understanding of the parameters; this explanation simplifies the process by focusing on the key steps and removing some of the more technical details. First, the prior information about the parameters will be estimated and expressed as a probability distribution. Next, the observed data is collected to update our prior beliefs and calculate the likelihood, which shows that the observed data is given different possible values of the parameters. Combining the preceding information and the observed data is called the posterior distribution. This distribution represents our updated belief about the parameters after considering the data. Using MCMC to estimate the posterior distribution can help sample data from the posterior distribution, allowing the estimation of the parameters more easily. Finally, the results of the MCMC sampling are used to estimate the parameters of the GEVD.

2.4. L-Moments method

L-moments [33] are statistical measures used to summarize the probability distributions of data. They offer a robust alternative to conventional moments for parameter estimation, which are linear combinations of order statistics. L-moments have several advantages over conventional moments, particularly their robustness to outliers and small sample sizes [34].

The approximation of L-moments can be arranged from the order statistics of the observed data in the following steps:

Step1: Calculate the sample L-moments (l_1, l_2, l_3) :

L-Mean: $l_1 = \frac{1}{n}\sum_{i=1}^{n} x_{(i)}$

L-Scale: $l_2 = \frac{1}{2}\left(\frac{2}{n}\sum_{i=1}^{n-1}\left(ix_{(i)} - (i-1)x_{(i-1)}\right)\right)$

L-Skewness: $l_3 = \frac{1}{3}\left(\frac{3}{n}\sum_{i=1}^{n-2}\left(i(i+1)x_{(i)} - 2i(i-1)x_{(i-1)} + (i-1)(i-2)x_{(i-2)}\right)\right)$

Step 2: Compute the L-moment ratios [35] (τ_2, τ_3), which are necessary for estimating the shape parameter (ξ) :

L-coefficient of variation $(\tau_2) = \frac{l_2}{l_1}$

L-skewness $(\tau_3) = \frac{l_3}{l_2}$

Step 3: Estimate the shape parameter ($\hat{\xi}$) by using the relationship between the third L-moment ratio (τ_3) and (ξ) :

$$\tau_3 = \frac{2\left(1 - 3^{-\xi}\right)}{1 - 2^{-\xi}} - 3$$

This equation is nonlinear and must be solved numerically for $\hat{\xi}$. A common approach is to use iterative methods such as the Newton-Raphson method.

Step 4: The Newton-Raphson method is used to estimate the shape parameter (ξ), it iteratively refines the parameter estimate until convergence. Let the function of the shape parameter $f(\xi) = 0$ represent the nonlinear equation for the shape parameter derived from the L-moments equations. Calculate the derivative of $f(\xi)$, denoted as $f'(\xi)$ which is necessary for the iterative updates in Newton-Raphson. Start with an initial guess for the shape parameter, ξ_0. This initial guess should be close to the expected value to ensure fast convergence.

Step 5: Using the Newton-Raphson formula, update the value of ξ iteratively as

$$\xi_{n+1} = \xi_n - \frac{f(\xi)}{f'(\xi)}$$

In each iteration, calculate the $f(\xi)$ and $f'(\xi)$ to update ξ_{n+1} by using the Newton-Raphson formula to compute the next estimate for ξ.

Step 6: Define a tolerance level $\varepsilon = 10^{-6}$ to determine when the iterative process should stop. The iteration continues until the difference between successive estimates of ξ is smaller than ε as $|\xi_{n+1} - \xi_n| < \varepsilon$. Once this criterion is met, the process has converged, and the current estimate ξ_{n+1} is accepted as the solution for the shape parameter.

Step 7: Estimate the shape parameter (σ) that can be calculated using the second L-moment (l_2) and the following relationship:

$$\hat{\sigma} = \frac{l_2\hat{\xi}}{\left(1-2^{-\hat{\xi}}\right)\Gamma(1+\hat{\xi})}$$

Step 8: Estimate the location parameter (μ) by using the first L-moment (l_1) and the following relationship:

$$\hat{\mu} = l_1 - \hat{\sigma}\left(1-\frac{\Gamma(1+\hat{\xi})}{\hat{\xi}}\right)$$

The L-moments method approach simplifies parameter estimation and provides reliable data distribution characterizations. It calculates L-moments such as L-mean, L-scale, and L-skewness to summarize the data's distribution. The shape, scale, and location parameters are then estimated using these L-moments, often with iterative methods like Newton-Raphson.

In terms of computational efficiency, the L-moments method offers a relatively faster approach than ML and Bayesian methods, as it relies on linear combinations of order statistics rather than solving complex likelihood equations. Nevertheless, iterative procedures can introduce additional computational burdens, especially when precision is crucial. Regarding error propagation, small sample sizes can lead to higher variability in the shape parameter estimates, affecting the accuracy of subsequent estimates of scale and location parameters.

Small sample sizes may also amplify the impact of rounding errors and numerical instability during the iterative estimation process, potentially resulting in biased estimates. To mitigate this, careful initial value selection and numerical techniques such as adaptive step-size adjustments and convergence checks are employed to ensure stable and reliable parameter estimation.

3. Simulation study and results

This section describes how to simulate data from a GEVD and presents the results in point estimation. The main focus of this study is to address the performance of parameter estimation, namely ML, GML, Bayesian, and L-moments methods. Through the Monte Carlo simulation, the study generated the random variable from the GEVD that encompassed three types of distributions: Weibull, Gumbel, and Fréchet distributions. The density characters of the three distributions are shown in Fig. 1.

From Fig. 1, the R program creates the GEVD with location parameter (μ) of three, a scale parameter (σ) of one, and the shape parameter for -0.7 (Weibull distribution), 0 (Gumbel distribution), and 0.7 (Fréchet distribution) on

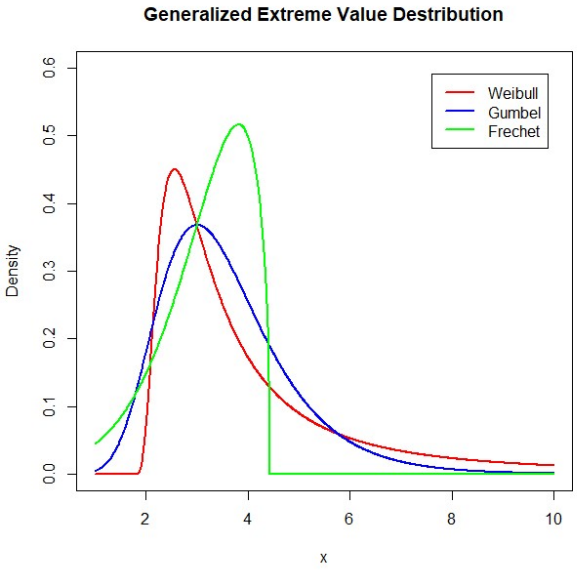

Fig. 1. GEVD with different shape parameters

1,000 replications. In setting the number of replications allowed for each algorithm to ensure that the simulation process is thorough and accurate, the convergence criteria are based on the change in parameter estimates between iterations. The computation will stop when the difference between successive parameter estimates is below a specified threshold, indicating that further changes in parameter estimates are minimal and the solution has stabilized. Early termination due to meeting convergence conditions ensures that the estimates are stable, enhancing the accuracy of MSE as a measure of estimator performance. The sample sizes (n) are 30, 50, 70, and 100. The extRemes 2.0 [36] package in R approximates parameters in GEVD on 1000 replications. The performance of the estimators ($\hat{\theta} = \hat{\mu}, \hat{\sigma}, \hat{\xi}$) is evaluated using minimum of mean square error criterion as follows:

$$\text{MSE}(\hat{\theta}) = \frac{\sum_{i=1}^{m}\left(\hat{\theta}_i - \theta\right)^2}{m}$$

In Table 1, the results show that ML outperforms for all parameters when the mean square error is minimal in all situations. The standard deviation values for each method and parameter are similar, and as the sample size increases, the standard deviation decreases. When the sample sizes increase, the MSE decreases, as shown in Fig. 2.

The lower MSE of ML in Table 1 can be attributed to the method's inherent statistical advantages, particularly its efficiency and ability to leverage likelihood-based estimation effectively. Additionally, the characteristics of the simulated dataset, including the controlled environment

Table 1. Estimating mean, standard deviation (SD) of estimated parameter, and mean square error with true parameter $\mu = 3, \sigma = 1$ and $\xi = -0.7$

n	Methods	Mean and SD of Estimated Parameter			Mean Square Error		
		Location (μ)	Scale (σ)	Shape (ξ)	Location (μ)	Scale (σ)	Shape (ξ)
30	ML	3.014 (0.222)	0.968 (0.231)	-0.713 (0.222)	0.0496	0.0544	0.0496
	GML	3.067 (0.245)	1.056 (0.297)	-0.545 (0.177)	0.0645	0.0915	0.0551
	Bayesian	3.077 (0.257)	1.169 (0.322)	-0.762 (0.223)	0.0721	0.1320	0.0538
	L-Moments	3.074 (0.244)	1.109 (0.322)	-0.517 (0.181)	0.0649	0.1154	0.0659
50	ML	3.006 (0.171)	0.974 (0.173)	-0.704 (0.174)	0.0292	0.0307	0.0303
	GML	3.040 (0.187)	1.051 (0.254)	-0.577 (0.129)	0.0365	0.0672	0.0316
	Bayesian	3.039 (0.180)	1.079 (0.200)	-0.725 (0.173)	0.0340	0.0464	0.0306
	L-Moments	3.052 (0.193)	1.093 (0.257)	-0.550 (0.162)	0.0399	0.0750	0.0483
70	ML	2.999 (0.137)	0.982 (0.145)	-0.714 (0.141)	0.0187	0.0213	0.0202
	GML	3.027 (0.161)	1.061 (0.251)	-0.597 (0.121)	0.0267	0.0667	0.0250
	Bayesian	3.026 (0.143)	1.055 (0.163)	-0.727 (0.141)	0.0212	0.0296	0.0206
	L-Moments	3.042 (0.166)	1.101 (0.254)	-0.577 (0.144)	0.0292	0.0748	0.0355
100	ML	3.001 (0.117)	0.987 (0.126))	-0.708 (0.111)	0.0136	0.0161	0.0123
	GML	3.031 (0.131)	1.054 (0.175)	-0.606 (0.108)	0.0181	0.0336	0.0204
	Bayesian	3.018 (0.120)	1.034 (0.135)	-0.715 (0.111)	0.0148	0.0194	0.0126
	L-Moments	3.042 (0.137)	1.085 (0.183)	-0.591 (0.129)	0.0204	0.0408	0.0284

Note: The underlined letter indicates the minimum mean square error.

and alignment with ML assumptions, further contribute to its superior performance. In practical applications, however, real-world complexities might influence the relative performance of different estimation methods.

The plots of Fig. 2 indicate that the ML method generally outperforms the other methods in terms of lower MSE across all parameters, especially as the sample size increases. The ML method consistently achieves lower MSE values, especially at larger sample sizes, indicating its efficiency in parameter estimation. The L-moments method tends to have higher MSE, particularly for smaller sample sizes, suggesting it may be less reliable under those conditions.

Table 2 shows that the minimum mean square error is reasonable for all methods with slightly different values. GML exhibited the minimum mean square, but Bayesian and L-moments methods outperformed in more than large sample sizes at the location parameter. The scale parameters of ML and GMLE perform well, and the GML method is robust in estimating the shape parameter. The standard deviation of the GML method is the lowest, and as the sample size increases, the standard deviation further decreases. The MSE decreases when samples increase, as shown in Fig. 3.

From Fig. 3, when the sample size increases, the differences in performance between the methods increase, with all methods showing low MSE at larger sample sizes. The ML and Bayesian methods perform well across all parameters, particularly in smaller sample sizes. The GML and L-moments methods also perform well but show slightly

Table 2. Estimating mean and standard deviation (SD) of estimated parameter and mean square error with true parameter $\mu = 3, \sigma = 1$, and $\xi = 0$

n	Methods	Mean and SD of Estimated Parameter			Mean Square Error		
		Location (μ)	Scale (σ)	Shape (ξ)	Location (μ)	Scale (σ)	Shape (ξ)
30	ML	3.017 (0.222)	0.966 (0.157)	0.008 (0.167)	0.0494	0.0258	0.0280
	GML	3.054 (0.208)	1.002 (0.153)	0.078 (0.079)	0.0460	0.0235	0.0122
	Bayesian	2.999 (0.222)	1.087 (0.177)	-0.055 (0.168)	0.0491	0.0389	0.0312
	L-Moments	3.002 (0.216)	0.993 (0.163)	-0.007 (0.140)	0.0465	0.0266	0.0197
50	ML	3.012 (0.160)	0.972 (0.122)	0.006 (0.124)	0.0256	0.0157	0.0153
	GML	3.044 (0.150)	1.000 (0.121)	0.067 (0.063)	0.0246	0.0146	0.0085
	Bayesian	3.002 (0.159)	1.036 (0.130)	-0.028 (0.122)	0.0254	0.0183	0.0157
	L-Moments	3.003 (0.158)	0.991 (0.129)	0.007 (0.114)	0.0249	0.0168	0.0131
70	ML	3.010 (0.139)	0.987 (0.099)	0.006 (0.099)	0.0193	0.0100	0.0099
	GML	3.037 (0.133)	1.008 (0.098)	0.056 (0.059)	0.0192	0.0097	0.0067
	Bayesian	3.003 (0.139)	1.030 (0.104)	-0.017 (0.098)	0.0192	0.0117	0.0100
	L-Moments	3.003 (0.138)	0.999 (0.105)	0.005 (0.097)	0.0191	0.0110	0.0094
100	ML	3.006 (0.110)	0.991 (0.081))	0.006 (0.076)	0.0121	0.0066	0.0058
	GML	3.029 (0.107)	1.008 (0.081)	0.047 (0.053)	0.0122	0.0067	0.0050
	Bayesian	3.002 (0.110)	1.020 (0.083)	-0.009 (0.076)	0.0120	0.0073	0.0058
	L-Moments	3.002 (0.110)	1.000 (0.086)	0.005 (0.077)	0.0121	0.0074	0.0060

Note: The underlined letter indicates the minimum mean square error.

higher MSE at smaller sample sizes in some cases.

Table 3 shows the location parameter has the minimum mean square error in the Bayesian and L-moments methods. The L-moments method has a performance method on the scale parameter, and the Bayesian outperforms in the shape parameter. In most cases, the Bayesian method provides the lowest standard deviation for the location and shape parameters. In contrast, the L-moments method gives the lowest standard deviation for the scale parameter. Fig. 4 shows the trending of MSE in all methods.

The ML method may experience instability or poor performance at specific sample sizes (notably around $n = 50$), as evidenced by the spikes in MSE shown in Fig. 4. In contrast, the GML, Bayesian, and L-moments methods demonstrate more stable and reliable performance, with the L-moments method generally showing the lowest MSE across all parameters. This suggests that the L-moments method may be the most robust and reliable across varying sample

In specific scenarios, Bayesian and GML methods may outperform ML, particularly in small sample sizes or when highly informative priors are available, helping stabilize estimates.

Including diagnostic comparisons, such as likelihood convergence and standard errors, can provide insights into why ML tends to have lower variability and higher accuracy. Additionally, discussing the trade-off between estimation accuracy and computational cost can help determine the most suitable method for practical applications, balancing precision with resource efficiency. sizes, particularly

Table 3. Estimating mean, standard deviation (SD) of estimated parameter, and mean square error with true parameter $\mu = 3, \sigma = 1$, and $\xi = 0.7$

n	Methods	Mean and SD of Estimated Parameter			Mean Square Error		
		Location (μ)	Scale (σ)	Shape (ξ)	Location (μ)	Scale (σ)	Shape (ξ)
30	ML	2.988 (0.246)	1.040 (0.435)	0.761 (0.328)	0.0607	0.1910	0.1116
	GML	2.932 (0.208)	0.927 (0.172)	0.576 (0.162)	0.0477	0.0347	0.0414
	Bayesian	2.929 (0.229)	1.032 (0.279)	0.649 (0.154)	0.0576	0.0786	<u>0.0263</u>
	L-Moments	2.979 (0.197)	0.950 (0.160)	0.644 (0.177)	<u>0.0390</u>	<u>0.0281</u>	0.0343
50	ML	2.997 (0.285)	1.044 (0.510)	0.745 (0.181)	0.0813	0.2619	0.0347
	GML	2.953 (0.187)	0.957 (0.143)	0.616 (0.113)	0.0369	0.0221	0.0197
	Bayesian	2.976 (0.160)	1.015 (0.150)	0.688 (0.108)	<u>0.0263</u>	0.0227	<u>0.0119</u>
	L-Moments	2.999 (0.163)	0.997 (0.130)	0.679 (0.136)	0.0264	<u>0.0174</u>	0.0189
70	ML	3.044 (0.148)	1.007 (0.232)	0.727 (0.106)	0.0220	0.0540	0.0120
	GML	2.944 (0.164)	0.975 (0.119)	0.619 (0.098)	0.0299	0.0148	0.0162
	Bayesian	2.975 (0.137)	1.014 (0.117)	0.692 (0.083)	0.0194	0.0138	<u>0.0070</u>
	L-Moments	2.984 (0.138)	0.987 (0.108)	0.673 (0.107)	<u>0.0193</u>	<u>0.0118</u>	0.0121
100	ML	2.984 (0.195)	1.046 (0.313))	0.735 (0.109)	0.0381	0.0998	0.0132
	GML	2.924 (0.232)	0.994 (0.150)	0.626 (0.093)	0.0593	0.0226	0.0142
	Bayesian	2.985 (0.111)	1.013 (0.102)	0.700 (0.069)	<u>0.0125</u>	0.0105	<u>0.0048</u>
	L-Moments	2.990 (0.112)	0.994 (0.091)	0.683 (0.090)	0.0126	<u>0.0082</u>	0.0084

Note: The underlined letter indicates the minimum mean square error.

when estimating location, scale, and shape parameters.

Tables 1 to 3 can summarize the key findings in Table 4.

The instability in maximum likelihood (ML) estimates at $n = 50$ can be attributed to several factors. Firstly, the small sample size may prevent the ML method from achieving reliable convergence, leading to higher variability in estimates, especially for complex distributions like the Generalized Extreme Value Distribution (GEVD), which may have multiple local optima. Secondly, the shape parameter (ξ) significantly affects the tail behavior of the distribution; when ξ is close to zero, the distribution approximates a Gumbel distribution, resulting in more stable estimates. However, large deviations in ξ, particularly in the Fréchet or Weibull cases, can make the likelihood function more sensitive to data fluctuations, causing estimation spikes. Thirdly, numerical convergence issues may arise due to the complexity of the likelihood equations, with iterative methods such as Newton-Raphson facing challenges in stability, possibly due to initial value selection or step sizes. Lastly, the bias-variance tradeoff is more pronounced in smaller samples, where ML estimation may exhibit higher variance. At the same time, methods like Bayesian or L-moments, which incorporate prior information, tend to provide more stable results.

4. Rainfall volume application

To evaluate the performance of the parameter estimation on extreme data, we utilized the rainfall volume data from Bangkok, the capital of Thailand, the largest city in the country, and served as its economic, cultural, and political

Table 4. The summarized strengths and limitations of parameter estimation methods

Method	Strengths	Limitations
Maximum Likelihood (ML)	Computationally efficient, performs well across sample sizes	High computational cost for large samples
Generalized Maximum Likelihood (GML)	Robust for moderate sample sizes, balances accuracy and computation time	Requires additional computational time
Bayesian	Incorporates prior knowledge, accurate for small samples	Computationally intensive, requires convergence diagnostics
L-Moments	Fast for large samples, does not require iterative optimization	Slightly higher MSE in smaller samples

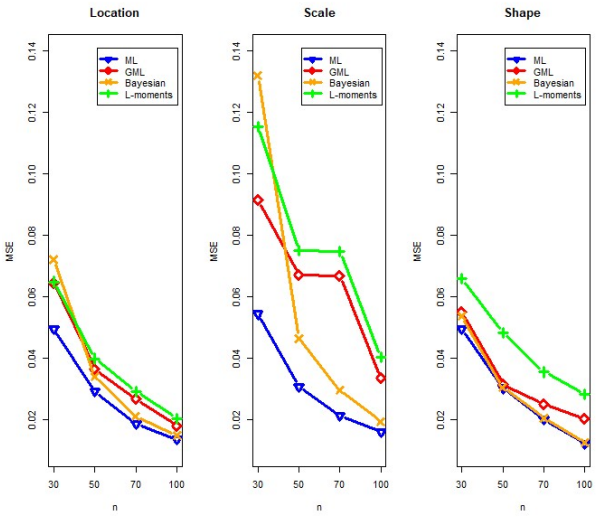

Fig. 2. The mean square error of parameter estimation with location, scale, and shape parameters as $\mu = 3, \sigma = 1$, and $\xi = -0.7$

center. The data was collected from Queen Sirikit National Convention Center (QSNCC) as station 1, Don Mueng district as station 2, Bang Na district as station 3, and Khlong Toei district as station 4. From this data, we selected the maximum yearly rainfall volume from 1994 to 2023 as 29 years. The data used in this research were obtained from daily rainfall records, measured in millimeters, from the website https://tmd.go.th/service/tmdData. After acquiring the data, the highest daily rainfall for each month was selected, followed by the highest monthly rainfall for each year. This data was then analyzed for the study.

Before the data analysis, the stationary data were checked using the Augmented Dickey-Fuller test [37] and the Mann-Kendall test [38]. The data from all four stations exhibited stationary characteristics. We employed ML, GML, Bayesian, and L-moments methods to approximate GEVD parameters for forecasting the return level over nine years.

To check the performance of parameter estimation, we used these estimated parameters to forecast the future value for estimating the confidence interval of the return level for nine years. The formula utilized for computing the return level:

$$\hat{x}_T = \hat{\mu} - \frac{\hat{\sigma}}{\hat{\xi}}\left\{1 - \left[-\log\left(1 - \frac{1}{T}\right)\right]^{-\hat{\xi}}\right\}, T = 2, 3, \ldots, 9$$

where is the location estimator, $\hat{\sigma}$ is the scale estimator, $\hat{\xi}$ is the shape estimator, and T is the return period.

The variance of the return level $(\hat{x}_t)$, using the Delta method [25], is given by:

$$\begin{aligned}\mathrm{Var}\,(x_T) \approx{}& \left(\frac{\partial g}{\partial \mu}\right)^2 \mathrm{Var}(\mu) + \left(\frac{\partial g}{\partial \sigma}\right)^2 \mathrm{Var}(\sigma) \\ &+ \left(\frac{\partial g}{\partial \xi}\right)^2 \mathrm{Var}(\xi) + 2\frac{\partial g}{\partial \mu}\frac{\partial g}{\partial \sigma}\mathrm{Cov}(\mu,\sigma) \\ &+ 2\frac{\partial g}{\partial \mu}\frac{\partial g}{\partial \xi}\mathrm{Cov}(\mu,\xi) + 2\frac{\partial g}{\partial \sigma}\frac{\partial g}{\partial \xi}\mathrm{Cov}(\sigma,\xi)\end{aligned}$$

The partial derivatives with respect to each parameter indicate the return level's sensitivity to changes in each parameter (μ, σ, ξ) following:

$$\frac{\partial g}{\partial \mu} = 1, \frac{\partial g}{\partial \sigma} = \frac{1}{\hat{\xi}}\left(\left(-\ln\left(1 - \frac{1}{T}\right)\right)^{-\hat{\xi}} - 1\right), \text{ and}$$

$$\begin{aligned}\frac{\partial g}{\partial \xi} = {}& -\frac{\hat{\sigma}}{\hat{\xi}^2}\left(\left(-\ln\left(1 - \frac{1}{T}\right)\right)^{-\xi} - 1\right) \\ &+ \frac{\hat{\sigma}}{\hat{\xi}}\ln\left(-\ln\left(1 - \frac{1}{T}\right)\right)\left(-\ln\left(1 - \frac{1}{T}\right)\right)^{-\hat{\xi}}\end{aligned}$$

To handle numerical instability in $\ln\left(1 - \frac{1}{T}\right)$ for extreme return periods, regularization techniques [25] like threshold limiting, Taylor series approximation, or rescaling the argument can be applied. Regularization techniques are used to address numerical instability in estimating return levels for extreme periods, such as threshold limiting, Taylor series approximation, and rescaling the

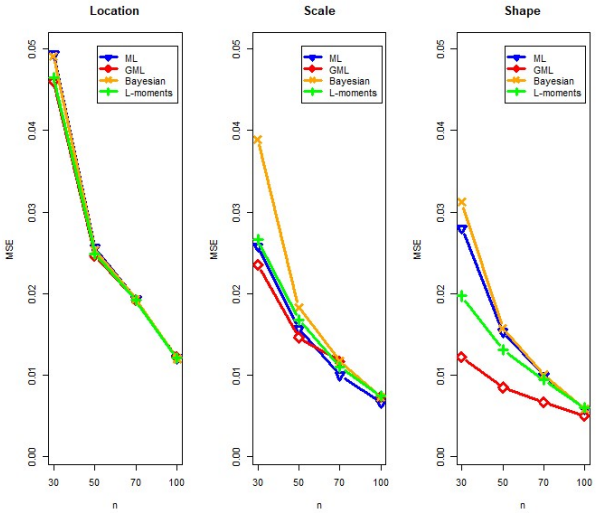

Fig. 3. The mean square error of parameter estimation with location, scale, and shape parameters as $\mu = 3, \sigma = 1$, and $\xi = 0$

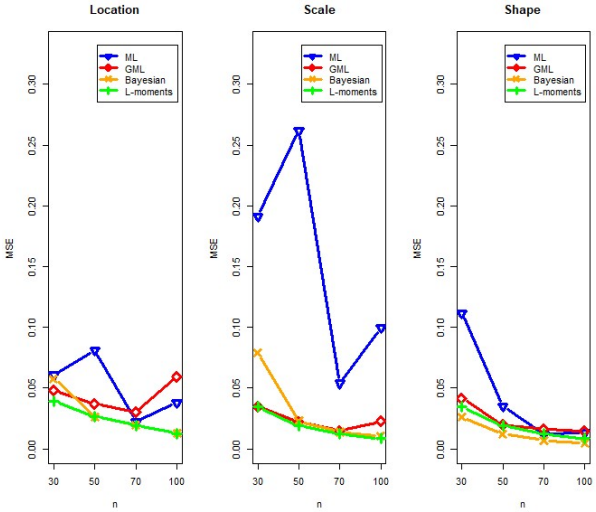

Fig. 4. The mean square error of parameter estimation with location, scale, and shape parameters as $\mu = 3, \sigma = 1$, and $\xi = 0.7$

argument. However, their impact on return-level estimates is not fully explained. To address this, a sensitivity analysis should assess how these techniques affect estimation accuracy, particularly for long return periods. Additionally, a comparison using metrics like Mean Absolute Percentage Error (MAPE) and confidence intervals can help evaluate their effectiveness, enhancing the clarity and reliability of the study. These methods prevent the logarithmic argument from approaching unstable values.

Additionally, higher-precision arithmetic ensures accuracy for small differences.

To compute the variances and covariance of the location (μ), scale (σ), and shape (ξ) parameters for the GEVD, the Bayesian analysis framework is typically employed to refine estimation techniques. This involves deriving posterior distributions for the parameters based on the observed data and prior distributions, often utilizing the inverse-gamma distribution for modeling the variance components. The computation uses Markov Chain Monte Carlo (MCMC) methods, such as the Metropolis-Hastings algorithm, to sample from the joint posterior distribution of μ, σ, and ξ. Then, the confidence interval is constructed by $\hat{x}_T \pm Z_{\alpha/2} \times \sqrt{\text{Var}\,(x_T)}$.

To compare the forecasting performance of the return level, MAPE (Mean Absolute Percentage Error), Root Mean Square Error (RMSE), and Mean Absolute error (MAE) will be used, which are approximated by

$$\text{Mean Absolute Percentage Error (MAPE)} = \frac{1}{9}\sum_{t=1}^{9}\left|\frac{x_t - \hat{x}_t}{x_t}\right| \times 100$$

$$\text{Root Mean Square Error (RMSE)} = \sqrt{\frac{1}{9}\sum_{t=1}^{9}(x_t - \hat{x}_t)^2},$$

$$\text{Mean Absolute Error (MAE)} = \frac{1}{9}\sum_{t=1}^{9}|x_t - \hat{x}_t|$$

where x_t is the real maximum rainfall volume and $\hat{x}_i$ is the estimated return level. We choose the minimum MAPE, RMSE, and MAE from all methods to exhibit in Table 5.

From Table 5, ML proposes a good performance at station 3, implying that the coefficient of skewness is almost the close value. On the other hand, the performance of GML in stations 1, 2, and 4 is proposed to have a higher coefficient of skewness than in station 3. The coefficient of skewness affects forecasting the return level. The values in parentheses represent the confidence intervals for the rainfall measurements at each station and return level. These intervals indicate the range within which the real rainfall amount is expected to fall with a certain confidence level.

The comparison shows that the estimated return levels generally fall within the 95% confidence intervals of observed values, demonstrating a reasonable model fit. ML performs well at Station 3, where skewness is low, while GML is more effective at stations with higher skewness. The variation in MAPE, RMSE, and MAE values across stations suggests that model performance depends on location-specific rainfall patterns. Notably, the lowest MAPE (32.57%), RMSE (35.08), and MAE (27.09) at Station 3 confirms the effectiveness of the ML method in less skewed data conditions.

Table 5. The real dataset of maximum rainfall volume and the estimated return levels (95% confidence interval) of Station 1, Station 2, Station 3, and Station 4

Return Level	Station 1 (SQQRS)		Station 2 (Don Mueng)		Station 3 (Bang Na)		Station 4 (Khlong Toei)	
	Maximum Rainfall	GML	Maximum Rainfall	GML	Maximum Rainfall	ML	Maximum Rainfall	GML
1	(95% Confidence) (Interval)		(95% Confidence) (Interval)		(95% Confidence) (Interval)		(95% Confidence) (Interval)	
2	60.3 (89.65, 119.22)	104.43	107.7 (90.53, 108.89)	99.71	91.6 (93.95, 100.01)	96.98	165.5 (82.04, 115.63)	98.83
3	174.3 (82.78, 154.21)	118.49	108.9 (89.44, 133.47)	111.45	92.9 (102.86, 119.15)	111.01	132.0 (69.28, 152.23)	110.76
4	141.5 (78.60, 176.04)	127.32	83.9 (88.87, 148.68)	118.77	119.0 (108.93, 132.65)	120.57	190.3 (61.08, 175. 75)	118.41
5	188.3 (75.61, 191.92)	133.76	93.2 (88.50, 159.68)	124.09	110.9 (113.61, 143.33)	128.47	152.5 (54.98, 193.18)	124.09
6	74.3 (73.30, 204.38)	138.84	65.0 (88.25, 168.27)	128.26	57.7 (117.46, 152.26)	134.86	62.2 (50.12, 207.09)	128.61
7	54.4 (71.42, 214.61)	143.02	78.6 (88.07, 175.31)	131.69	88.0 (120.75, 159.99)	140.37	103.4 (46.07, 218.66)	132.36
8	118.0 (69.84, 223.29)	14657	62.2 (87.93, 181.26)	134.59	120.9 (123.62, 166.83)	145.23	108.4 (42.60, 228.56)	135.58
9	132.5 (68.49, 230.82)	149.65	74.9 (87.82, 186.40)	137.11	126.0 (126.17, 172.99)	149.58	130.3 (39.57, 237.23)	138.40
10	87.2 (67.30, 237.45)	152.38	53.0 (87.73, 190.93)	139.33	129.8 (128.48, 178.61)	153.55	74.8 (36.87, 244.93)	140.90
MAPE	-	56.92	-	40.08	-	32.57	-	40.80
RMSE	-	53.34	-	53.35	-	35.08	-	48.64
MAE	-	48.08	-	45.93	-	27.09	-	42.77

Note: The underlined letter indicates the minimum MAPE, RMSE, and MAE

A comparison of forecasted versus observed extreme rainfall values shows that the predicted return levels for shorter return periods (2 to 5 years) align well with historical extremes, demonstrating the reliability of the estimation methods. However, specific years reveal anomalies where observed rainfall exceeds predictions, likely due to climate change, localized weather patterns, or changes in land use impacting runoff.

Accurate return-level estimates of extreme rainfall events help city planners design drainage systems that can handle peak rainfall levels, preventing system overload. These estimates support flood mitigation strategies and aid policymakers in improving emergency preparedness by setting early warning thresholds and allocating resources efficiently. Incorporating return-level data into urban planning ensures proper stormwater management and zoning regulations in flood-prone areas.

5. Discussions

The application of GEVD in forecasting maximum rainfall volume for Bangkok has provided significant insights into the city's extreme weather patterns and the methodologies for their analysis. This study's findings underscore the effectiveness of the GEVD in capturing the characteristics of extreme rainfall events, which is crucial for urban planning, infrastructure development, and disaster risk management [39].

The results are obtained from estimating a parameter of the GEVD distribution to the Weibull, Gumbel, and Fréchet distributions. Firstly, the parameter estimation methods used in this study, namely Maximum Likelihood (ML), Generalized Maximum Likelihood (GML), Bayesian Estimation, and L-moments that each methods have their strengths and limitations. ML method, in particular, provides robust frameworks for parameter estimation, enabling the accurate modeling of extreme events in Weibull distribution.

The GML method also proves effective due to its resistance to Gumbel distribution and straightforward computation for small sample sizes. For Fréchet distribution, Bayesian and L-moments methods perform the performance method in robust estimating parameters. Considering the standard deviation of each method, it was found that as the sample size increases, the standard deviation decreases. This leads to the conclusion that the estimation methods are consistent and suitable for parameter estimation. The results from both the simulated data and real data studies indicate that the methods used for parameter estimation yield consistent outcomes.

The findings of this study align with previous research on using GEVD for extreme value analysis in hydrological studies. Similar studies have demonstrated the GEVD's capability to model extreme precipitation events and its application in assessing flood risks and managing water resources. By comparing the GEVD under a stationary process with different parameter estimation methods, this study contributes to the broader literature by providing a detailed analysis of Bangkok's climatic context.

The ability to forecast maximum rainfall volumes at various return levels is precious for urban resilience planning. Accurate predictions of extreme rainfall events enable city planners and policymakers to design effective drainage systems, enhance flood protection measures, and develop emergency response strategies. Given the increasing variability in weather patterns due to climate change, the insights gained from this study are timely and critical.

The ML method demonstrated strong performance by efficiently handling the large sample size and providing accurate parameter estimates for the distribution types in the rainfall data [13]. While robust, the GML method showed limitations with small sample sizes, which may have affected its performance [22]. On the other hand, the Bayesian method effectively captured the uncertainty in parameter estimates, especially in the presence of skewed distributions, which were evident in some of the data points [40]. The L-moments method, known for its robustness to outliers and efficiency with small samples, performed well when the data exhibited high variability [41]. These variations in performance across methods underscore the importance of choosing the appropriate estimation technique based on the data's specific characteristics, such as sample size, distribution type, and the presence of outliers.

Future research could expand on this study by exploring the impact of non-stationarity in climate data, incorporating climate change scenarios into the generalized extreme value analysis, and applying the methodology to other urban areas prone to extreme weather events. Additionally, integrating other statistical models and machine learning techniques with the GEVD could enhance extreme value analysis's predictive accuracy and reliability. These limitations suggest areas for future research, including expanding the geographical scope, considering non-stationary models, and exploring additional estimation methods to improve the robustness and applicability of the findings.

In conclusion, using the GEVD in forecasting maximum rainfall volumes for Bangkok has demonstrated its effectiveness and provided valuable insights for managing extreme weather risks [42]. It can also serve as a guideline for forecasting maximum rainfall in other cities, such as Guwahati, India [43] and Thessaloniki, Greece [44], to plan urban management appropriate for the expected water volume. The methodologies and findings presented in this study offer a robust framework for future research and practical applications in urban planning and disaster risk management.

The study's findings offer critical insights into Bangkok's extreme rainfall patterns, which are essential for effective flood management. These results enable urban planners and policymakers to improve flood resilience through better drainage system design, accurate emergency preparedness forecasting and informed urban development decision-making. By incorporating this data into planning, Bangkok can enhance its infrastructure's ability to handle extreme weather, reduce flood risks, and contribute to the city's long-term sustainability and climate change.

Climate change introduces trends, shifts, and increased variability in rainfall patterns, making the assumption of stationarity less valid and potentially leading to inaccurate risk assessments. To address non-stationarity, methods such as time-varying parameters that adapt to evolving climate conditions, non-stationary GEV models incorporating climate covariates, and machine learning techniques to detect complex rainfall patterns can be employed. Additionally, Bayesian approaches provide a framework to integrate prior knowledge and account for uncertainties in climate trends, improving the robustness of parameter estimation.

6. Conclusions

This study explored various methods for parameter estimation of the GEVD, focusing on their application in forecasting the maximum rainfall volume in Bangkok, Thailand. The critical methods investigated included ML, GML, Bayesian, and L-moments. Each method was evaluated based on its ability to provide accurate point estimates for the GEVD parameters, including location, scale, and shape. The shape parameter can be verified in Weibull, Gumbel,

and Fréchet distributions. The simulation study provided valuable insights into the performance of these estimation methods. ML demonstrated robust performance in terms of accuracy and computational efficiency, particularly with Weibull distribution. GML and L-moments showed their utility in Gumbel distribution. L-moments and Bayesian offers valuable guidance on Fréchet distribution. Applying these methods to the annual maximum rainfall data for Bangkok from 1993 to 2023, the study highlighted the practicality of GEVD in modeling extreme rainfall events. The analysis indicated that the GML and ML could effectively capture the variability of extreme rainfall, providing reliable estimates for return levels over different periods. This capability is crucial for urban planning, flood management, and disaster preparedness in regions prone to extreme weather events.

In future research, climate change scenarios can be integrated into extreme value analysis using non-stationary models that allow parameters to vary over time in response to changing climatic conditions. Hybrid approaches combining machine learning techniques, such as neural networks and random forests, with GEVD could enhance predictive performance. Additional climate-related covariates, such as temperature and humidity, may improve return level estimates. This approach incorporates climate projections from global or regional climate models to simulate future rainfall patterns under various scenarios. By modeling GEVD parameters like location, scale, and shape as functions of time or other climate-related factors, the analysis can more accurately predict the impact of climate change on extreme rainfall events. This will enhance the relevance and accuracy of predictions, benefiting future urban planning and flood management in Bangkok or other countries.

7. Acknowledgments

This work was financially supported by King Mongkut's Institute of Technology Ladkrabang [KREF016703].

References

[1] G. Casella and R. L. Berger. *Statistical Inference*. 2nd. California: The Wadsworth Group, 2001. Chap. 7.

[2] C. C. Holms and S. G. Walker, (2003) *"Statistical Inference with Exchangeability and Martingales"* **Philosophical Transactions of the Royal Society A** ***381***: 1–17. DOI: 10.1098/rsta.2022.0143.

[3] J. Siebert, (2023) *"Applications of Statistical Causal Inference in Software Engineering"* **Information and Software Technology** ***159***: 1–34. DOI: 10.1016/j.infsof.2023.107198.

[4] T. T. Cal, Z. Gua, and R. Ma, (2023) *"Statistical Inference for High-Dimensional Generalized Linear Models with Binary Outcomes"* **Journal of the American Statistical Association** ***118***: 1319–1332. DOI: 10.1080/01621459.2021.1990769.

[5] C. H. Chong, M. Hoffmann, Y. Liu, M. Rosenbaum, and G. Szymanski, (2024) *"Statistical Inference for Rough Volatility: Central Limit Theorems"* **The Annals of Applied Probability** ***34***: 2600–2649. DOI: 10.1214/23-AAP2002.

[6] J. L. Wadsworth and R. Campbell, (2024) *"Statistical Inference for Multivariate Extremes via a Geometric Approach"* **Journal of the Royal Statistical Society Series B: Statistical Methodology** ***86***: 1243–1265. DOI: 10.1093/jrsssb/qkae030.

[7] P. C. Bellec and C.-H. Zhang, (2023) *"Debiasing Convex Regularized Estimators and Interval Estimation in Linear Models"* **The Annals of Statistics** ***51***: 391–436. DOI: 10.1214/22-AOS2243.

[8] C. Shi, J. Zhu, Y. Shen, S. Luo, H. Zhu, and R. Song, (2024) *"Off-Policy Confidence Interval Estimation with Confounded Markov Decision Process"* **Journal of the American Statistical Association** ***119***: 273–284. DOI: 10.1080/01621459.2022.2110878.

[9] S. F. Cheung, I. J. Agaloos Pesigan, and W. N. Vong, (2023) *"DIY Bootstrapping: Getting the Nonparametric Bootstrap Confidence Interval in SPSS for any Statistics or Function of Statistics"* **Behavior Research Methods** ***55***: 474–490. DOI: 10.3758/s13428-022-01808-5.

[10] L. Makkonen and M. Tikanmaki, (2019) *"An Improved Method of Extreme Value Analysis"* **Journal of Hydrology 2**: 1–7. DOI: 10.1016/j.hydroa.2018.100012.

[11] H. Tabari, (2021) *"Extreme Value Analysis Dilemma for Climate Change Impact Assessment on Global Flood and Extreme Precipitation"* **Journal of Hydrology** ***593***: 1–56. DOI: 10.1016/j.jhydrol.2020.125932.

[12] R. Raiman, S. Sukono, S. Supian, and N. Ismail, (2021) *"Analysing the Decision Making for Agricultural Risk Assessment: An Application of Extreme Value Theory"* **Decision Science Letters** ***10***: 351–360. DOI: 10.5267/j.dsl.2021.2.003.

[13] F. D. Paola, M. Giugni, F. Pugliese, A. Annis, and F. Nardi, (2018) *"GEV Parameter Estimation and Stationary vs. Non-Stationary Analysis of Extreme Rainfall in African Test Cities"* **Hydrology** ***5***: 1–23. DOI: 10.3390/hydrology5020028.

[14] S. Yoon, W. Cho, J.-H. Heo, and C. E. Kim, (2010) *"A Full Bayesian Approach to Generalized Maximum Likelihood Estimation of Generalized Extreme Value Distribution"* **Stochastic Environmental Research and Risk Assessment** ***24***: 761–770. DOI: 10.1007/s00477-009-0362-7.

[15] A. Shabri, U. N. Ahmad, and Z. A. Zakaria, (2011) *"TL-Moments and L-Moments Estimation of the Generalized Logistic Distribution"* **Journal of Mathematics Research** ***3***: 97–106. DOI: 10.5539/jmr.v3n1p97.

[16] S. B. Habeeb, F. K. Abdullah, R. N. Shalan, A. S. Hassan, E. M. Almetwally, F. M. Alghamdi, S. M. Ahmed Alsheikh, and M. Hossain, (2024) *"Comparison of Some Bayesian Estimation Methods for Type-I Generalized Extreme Value Distribution with Simulation"* **Alexandria Engineering Journal** ***98***: 356–363. DOI: 10.1016/j.aej.2024.04.042.

[17] Y. Ali, S. Washington, and M. Haque, (2023) *"Estimating Real-Time Crash Risk at Signalized Intersections: A Bayesian Generalized Extreme Value Approach"* **Safety Science** ***164***: 1–9. DOI: 10.1016/j.ssci.2023.106181.

[18] A. Louzaoui and M. E. Arrouchi, (2020) *"On the Maximum Likelihood Estimation of Extreme Value Index Based on k-Record Values"* **Journal of Probability and Statistics** ***2020***: 1–9. DOI: 10.1155/2020/5497413.

[19] S. E. Adlouni, T. B. Ouarda, X. Zhang, R. Roy, and B. Bobée, (2007) *"Generalized Maximum Likelihood Estimators for the Nonstationary Generalized Extreme Value Model"* **Water Resources Research** ***43***(3): 1–14. DOI: 10.1029/2005WR004545.

[20] F. Krüger, S. Lerch, T. Thorarinsdottir, and T. Gneiting, (2021) *"Predictive Inference based on Markov Chain Monte Carlo Output"* **International Statistical Review** ***89***: 274–301. DOI: 10.1111/insr.12405.

[21] S. A. Khan, I. Hussain, T. Hussain, F. Muhammad, Y. S. Muhammad, and A. M. Shoukry, (2017) *"Regional Frequency Analysis of Extremes Precipitation using L-Moments and Partial L- moments"* **Advances in Meteorology** ***2017***: 1–20. DOI: 10.1155/2017/6954902.

[22] E. Tanprayoon, U. Tonggumnead, and S. Aryuyuen, (2023) *"New Extension of Generalized Extreme Value Distribution: Extreme Value Analysis and Return Level Estimation of the Rainfall Data"* **Trends in Sciences** ***20***: 1–13. DOI: 10.48048/tis.2023.4034.

[23] E. S. Martins and J. R. Stedinger, (2000) *"Generalized Maximum-Likelihood Generalized Extreme-Value Quantile Estimators for Hydrologic Data"* **Water Resources Research** ***36***: 737–744. DOI: 10.1029/1999WR900330.

[24] J. L. Ng, K. H. Chan, N. I. F. Noh, R. Razman, S. Surol, J. C. Lee, and R. A. Al-Mansob, (2022) *"Statistical Modelling of Extreme Temperature in Peninsular Malaysia"* **IOP Conference Series: Earth and Environmental Science** ***1022***: 1–9. DOI: 10.1088/1755-1315/1022/1/012072.

[25] S. Coles. *An Introduction to Statistical Modeling of Extreme Values*. London: Springer, 2001. Chap. 1.

[26] J. Beirlant, Y. Goegebeur, J. Teugels, and J. Segers. *Statistics of Extremes: Theory and Applications*. New York: John Wiley & Sons, 2004. Chap. 1.

[27] J. Nocedal and S. J. Wright. *Numerical Optimization*. 2nd. New York: Springer, 1999. Chap. 1.

[28] E. Greenshtein and Y. Ritov, (2022) *"Generalized Maximum Likelihood Estimation of the Mean of Parameters of Mixtures, with Applications to Sampling and to Observational Studies"* **Electronic Journal of Statistics** ***16***: 5934–5954. DOI: 10.1214/22-EJS2082.

[29] S. Brooks, (2002) *"Markov Chain Monte Carlo Method and its Application"* **Journal of the Royal Statistical Society: Series D (the Statistician)** ***47***: 69–100. DOI: 10.1111/1467-9884.00117.

[30] S. Chib and E. Greenberg, (1995) *"Understanding the Metropolis-Hastings Algorithm"* **The American Statistician** ***49***(4): 327–335. DOI: 10.1080/00031305.1995.10476177.

[31] A. Gelman, J. B. Carlin, H. S. Stern, D. B. Dunson, A. Vehtari, and D. B. Rubin. *Bayesian Data Analysis*. 3rd. Florida: CRC Press Taylor & Francis Group, 2013. Chap. 2.

[32] A. Gelman and D. B. Rubin, (1992) *"Inference from Iterative Simulation Using Multiple Sequences"* **Statistical Science** ***7***: 457–472. DOI: 10.1214/ss/1177011136.

[33] J. R. M. Hosking, (1990) *"L-moments: Analysis and Estimation Distributions using Linear Combinations of Order Statistics"* **Journal of the Royal Statistical Society Series B: Statistical** ***52***: 105–124. DOI: 10.1111/j.2517-6161.1990.tb01775.x.

[34] E. A. H. Elamir and A. H. Seheult, (2004) *"Exact Variance Structure of Sample L-moments"* **Journal of Statistical Planning and Inference *124***: 337–359. DOI: 10.1016/S0378-3758(03)00213-1.

[35] J. Karvanen, (2006) *"Estimation of Quantile Mixtures via L-Moments and Trimmed L-moments"* **Computational Statistics & Data Analysis *51***: 947–959. DOI: 10.1016/j.csda.2005.09.014.

[36] E. Gilland and R. W. Katz, (2016) *"extRems 2.0: An Extreme Value Analysis Package in R"* **Journal of Statistical Software *72***: 1–39. DOI: https://doi.org/10.18637/jss.v072.i08.

[37] D. A. Dickey and W. A. Fuller, (1979) *"Distribution of the Estimators for Autoregressive Time Series with a Unit Root"* **Journal of the American Statistical Association *74***: 427–431. DOI: 10.1080/01621459.1979.10482531.

[38] R. M. Hirsch, J. R. Slack, and R. A. Smith, (1982) *"Techniques of Trend Analysis for Monthly Water Quality Data"* **Water Resources Research *18***: 107–121. DOI: 10.1029/WR018i001p00107.

[39] T. R. Ferreira, G. R. Liska, and L. A. Beijo, (2024) *"Assessment of Alternative Methods for Analysing Maximum Rainfall Spatial Data based on Generalized Extreme Value Distribution"* **Discover Applied Science *6***: 1–21. DOI: https://doi.org/10.1007/s42452-024-05685-9.

[40] Z. Jiao, A. Alam, J. Yuan, C. Farnham, and K. Emura, (2024) *"Prediction of Extreme Rainfall Events in 21st Century - The results Based on Bayesian Markov Chain Monte Carlo"* **Urban Climate *53***: 1–13. DOI: 10.1016/j.uclim.2024.101822.

[41] S. H. Lee and S. J. Maeng, (2005) *"Estimating of Drought Rainfall using L-Moments"* **Irrigation and Drainage *54***: 279–294. DOI: 10.1002/ird.178.

[42] T. Prahadchai, Y. Shin, P. Busababodhin, and J.-S. Park, (2023) *"Analysis of Maximum Precipitation in Thailand using Non-Stationary Extreme Value Models"* **Atmospheric Science Letters *24***: 1–11. DOI: 10.1002/asl.1145.

[43] R. Choudury and T. D. Roy, (2024) *"Rainfall Analysis of Guwahati City using the Method of L-Moments, Tl-Moments & Maximum Likelihood Estimation"* **International Journal of Scientific Research in Multidisciplinary Studies *10***: 19–25. DOI: 10.26438/ijsrms/v10i5.1925.

[44] I. Christos, P. Galiatsatou, V. Glenis, P. Prinos, and C. Kilsby, (2023) *"Urban Flood Modelling under Extreme Rainfall Conditions for Building-Level Flood Exposure Analysis"* **Hydrology *10***: 1–19. DOI: 10.3390/hydrology10080172.